Dynamical generation of the scalar $f_0(500)$, $f_0(980)$ and $K_0^*(700)$ resonances in the $D_s^+ \to K^+\pi^+\pi^-$ reaction

Lianrong Dai

Huzhou University, Zhejiang, China

QNP, July 8-12, 2024, University of Barcelona
The 10th International Conference on Quarks and Nuclear Physics

LRD & E. Oset, Phys. Rev. D 109 (2024) 054008

Motivation

The $D_s \to K^+\pi^+\pi^-$ decay reaction has been measured by the FOCUS collaboration [PLB601(2004)10] and BESIII collaboration [JHEP08(2022)196] with better statistics.

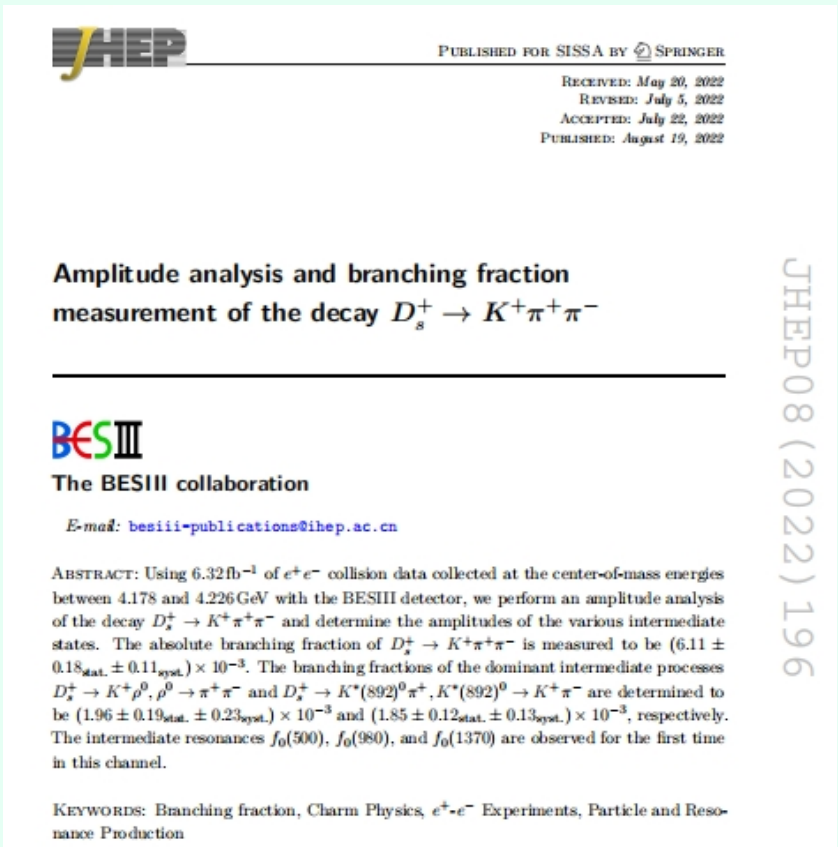

JHEP

Published for SISSA by Springer

Received: May 20, 2022
Revised: July 5, 2022
Accepted: July 22, 2022
Published: August 19, 2022

Amplitude analysis and branching fraction measurement of the decay $D_s^+ \to K^+\pi^+\pi^-$

BESIII

The BESIII collaboration

E-mail: besiii-publications@ihep.ac.cn

Abstract: Using 6.32 fb^{-1} of e^+e^- collision data collected at the center-of-mass energies between 4.178 and 4.226 GeV with the BESIII detector, we perform an amplitude analysis of the decay $D_s^+ \to K^+\pi^+\pi^-$ and determine the amplitudes of the various intermediate states. The absolute branching fraction of $D_s^+ \to K^+\pi^+\pi^-$ is measured to be $(6.11 \pm 0.18_{\rm stat.} \pm 0.11_{\rm syst.}) \times 10^{-3}$. The branching fractions of the dominant intermediate processes $D_s^+ \to K^+\rho^0, \rho^0 \to \pi^+\pi^-$ and $D_s^+ \to K^*(892)^0\pi^+, K^*(892)^0 \to K^+\pi^-$ are determined to be $(1.96 \pm 0.19_{\rm stat.} \pm 0.23_{\rm syst.}) \times 10^{-3}$ and $(1.85 \pm 0.12_{\rm stat.} \pm 0.13_{\rm syst.}) \times 10^{-3}$, respectively. The intermediate resonances $f_0(500)$, $f_0(980)$, and $f_0(1370)$ are observed for the first time in this channel.

Keywords: Branching fraction, Charm Physics, e^+-e^- Experiments, Particle and Resonance Production

JHEP08(2022)196

We study the singly Cabibbo-suppressed $D_s \to K^+\pi^+\pi^-$ decay.

In addition to the dominant mode $D_s^+ \to K^+\rho$, $\rho \to \pi^+\pi^-$ and $D_s^+ \to K^*(892)^0\pi^+$, $K^*(892)^0 \to K^+\pi^-$,

the experiment finds traces of the $f_0(500)$, $f_0(980)$ and $f_0(1370)$ resonances.

No theoretical work on this particular channel is available to the best of our knowledge, and we wish to address this problem here.

in the present work our aim

1) We relate the production of the $f_0(500)$, $f_0(980)$ and $K_0^*(700)$ scalar resonances by the chiral unitary approach [Oller, Oset, Ramos, Prog Part Nucl Phys 45(2000) 157]
2) One looks at the main production modes at the quark level based on external emission and internal emission [Chau, Phys Rept 95 (1983) 1], and then proceeds with the hadronization of the $q\bar{q}$ pairs in order to produce the coupled channels needed to generate these resonances.
3) The nice thing is that we can correlate the production of these resonances by means of only one parameter.
4) This procedure is different from the experimental analyses where the production of each of these resonances is parametrized and fitted to the data.

Our approach is very restrictive, and the eventual agreement with the data comes to **support the picture** of these resonances as being dynamically generated from the interaction of pseudoscalar mesons.

Formalism

At first, at the quark level, we look at the different topologies that can contribute to this Cabibbo-suppressed process.

Fig. 1 produce a π^+ and K^{*0} with external emission, and $K^{*0} \to K^+\pi^-$, one important modes observed in the BESIII experiment [JHEP08(2022)196]

Fig. 2 produce a ρ^0 meson and a K^+, and the $\rho^0 \to \pi^+\pi^-$, again one important mode observed in the BESIII experiment [JHEP08(2022)196]

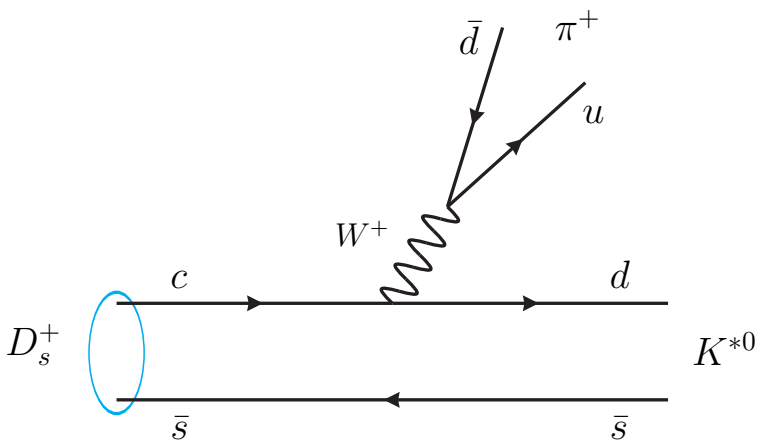

Fig. 1. Mechanism for production of π^+K^{*0} in D_s^+ decay with external emission

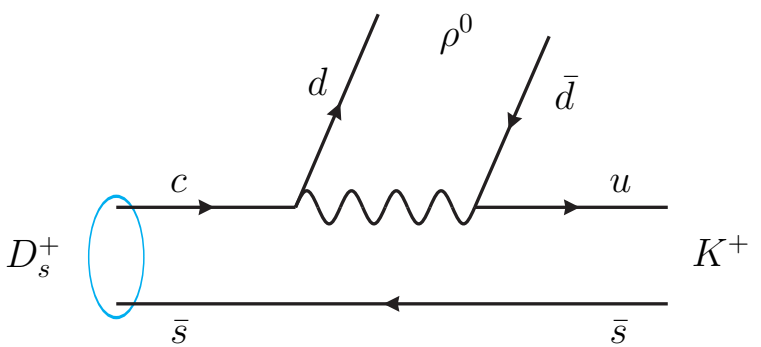

Fig. 2. Mechanism for $D_s^+ \to \rho K^+$ with internal emission

Hadronization of $q\bar{q}$ component

Next we look at the **production of three pseudoscalar mesons**. This is accomplished by **hadronizing a $q\bar{q}$ component** into two pseudoscalar mesons.

Fig. 3 a K^+ is produced in external emission and the $s\bar{s}$ component is hadronized into two pseudoscalars.
the Cabibbo-suppressed $W\bar{s}u$ vertex appears in the upper part

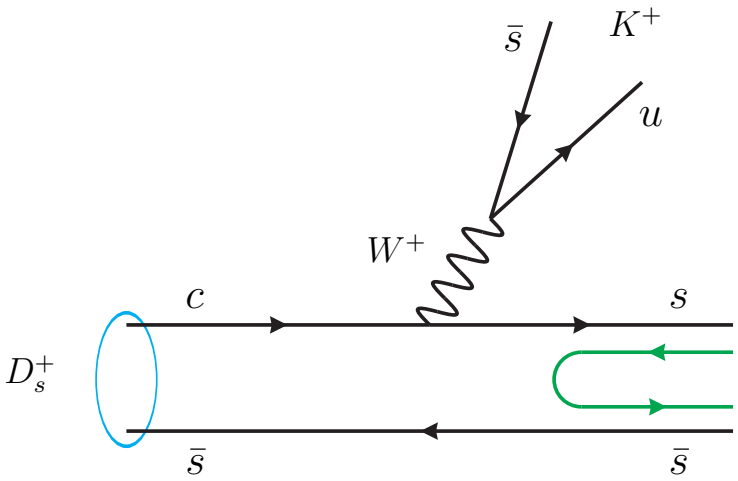

Fig. 3. $D_s^+ \to K^+ s\bar{s}$ with external emission and $s\bar{s}$ hadronization

Fig. 4 again with external emission, a π^+ is produced and the $d\bar{s}$ component is hadronized into two pseudoscalars.
the Cabibbo-suppressed $Wc\bar{d}$ vertex appears in the lower part

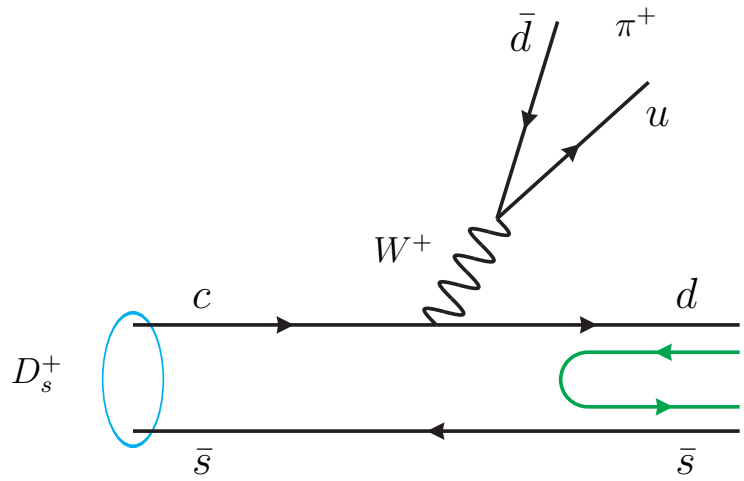

Fig. 4. $D_s^+ \to \pi^+ d\bar{s}$ with external emission and $d\bar{s}$ hadronization

Both vertices imply the same reduction factor

Both vertices imply the same factor $\sin\theta_c$

Fig. 5 the mechanism proceeds via internal emission, a K^+ is produced and the $s\bar{s}$ component is hadronized into two pseudoscalars.

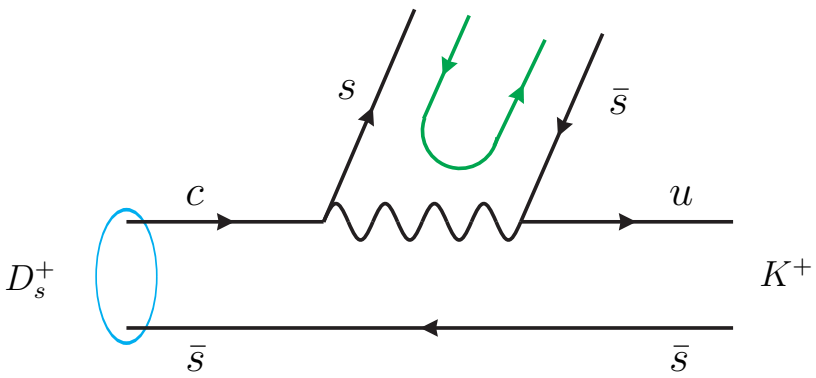

Fig. 5. $D_s^+ \to K^+ s\bar{s}$ with internal emission followed by $s\bar{s}$ hadronization

Fig. 6 again with internal emission a K^+ is produced and the $d\bar{d}$ component is hadronized into two pseudoscalars.

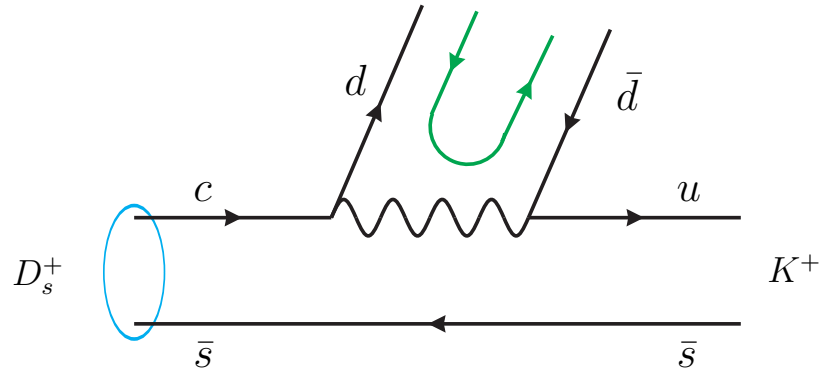

Fig. 6. $D_s^+ \to K^+ d\bar{d}$ with internal emission and $d\bar{d}$ hadronization

Table 1: The weight to the different diagrams

	Fig. 1	Fig. 2	Fig. 3	Fig. 4	Fig. 5	Fig. 6
weight	α	γ	$\alpha\ h$	$\alpha\ h$	$\gamma\ h$	$\gamma\ h$

h factor accounting for the mechanism of hadronization

For different hadronization processes

$\Longrightarrow$ add a $\bar{q}q$ pair with the quantum numbers of the vaccum.

By writing the $q_i\bar{q}_j$ matrix of SU(3) in terms of the pseudoscalar mesons

$$q\bar{q} \to P = \begin{pmatrix} \frac{\pi^0}{\sqrt{2}} + \frac{\eta}{\sqrt{3}} & \pi^+ & K^+ \\ \pi^- & -\frac{\pi^0}{\sqrt{2}} + \frac{\eta}{\sqrt{3}} & K^0 \\ K^- & \bar{K}^0 & -\frac{\eta}{\sqrt{3}} \end{pmatrix} \tag{1}$$

Then we have the different hadronization

$$s\bar{s} \to \sum_i s\,\bar{q}_i q_i\,\bar{s} = \sum_i P_{3i}P_{i3} = (P^2)_{33} = K^-K^+ + \bar{K}^0K^0 + \frac{1}{3}\eta\eta$$

$$d\bar{s} \to \sum_i d\,\bar{q}_i q_i\,\bar{s} = \sum_i P_{2i}P_{i3} = (P^2)_{23} = \pi^-K^+ - \frac{1}{\sqrt{2}}\pi^0K^0$$

$$d\bar{d} \to \sum_i d\,\bar{q}_i q_i\,\bar{d} = (P^2)_{22} = \pi^-\pi^+ + \frac{\pi^0\pi^0}{\sqrt{2}} + \frac{\eta\eta}{3} - \frac{2}{\sqrt{6}}\pi^0\eta + K^0\bar{K}^0 \tag{2}$$

$$5)+6) \to (P^2)_{33} + (P^2)_{22} = \pi^+\pi^- + \frac{\pi^0\pi^0}{\sqrt{2}} + \frac{2}{3}\eta\eta + K^+K^- + 2K^0\bar{K}^0 - \sqrt{\frac{2}{3}}\pi^0\eta \qquad (3)$$

We can see that in Fig. 6 we already obtain $K^+\pi^-\pi^+$ at the tree level, but we also get other intermediate states that upon rescattering lead to the same state, as depicted in Fig. 7

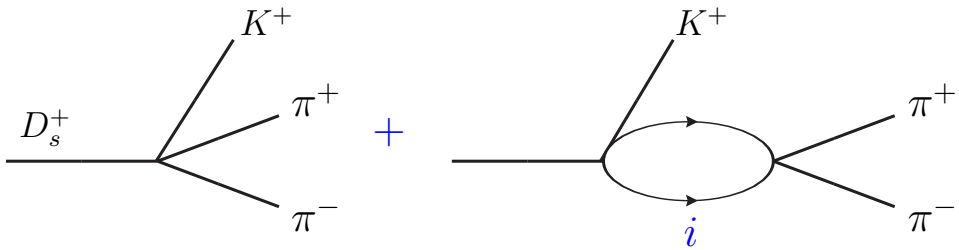

Fig. 7. Direct $K^+\pi^-\pi^+$ production (tree level) and production through intermediate states, $i = \pi^+\pi^-$, $\pi^0\pi^0$, $\eta\eta$, $\pi^0\eta$, K^+K^-, $K^0\bar{K}^0$ in general.

we can write the production matrix for each mechanism

$$t^{(3)} = \sum_i \alpha\, h\, W_i\, G_i\, t_{i,\pi^+\pi^-} \qquad \textbf{(Fig. 3)}$$

where G_i are the meson-meson loop functions and $t_{i,\pi^+\pi^-}$ the scattering matrices for transitions of the state i in the loop to the $\pi^+\pi^-$ final state.

The intermediate states: $i = K^+K^-, K^0\bar{K}^0, \eta\eta$, weights $W_{K^+K^-} = 1$, $W_{K^0\bar{K}^0} = 1$, $W_{\eta\eta} = \frac{2}{3}\frac{1}{\sqrt{2}}$

The loop function calculated with cut off regularization

$$G(s) = \int_{|\boldsymbol{q}|<q_{\max}} \frac{d^3q}{(2\pi)^3} \frac{\omega_1+\omega_2}{2\,\omega_1\,\omega_2} \frac{1}{s-(\omega_1+\omega_2)^2+i\epsilon} \tag{4-a}$$

where $\omega_j = \sqrt{\boldsymbol{q}^2 + m_j^2}$ calculated for each channel, using $q_{\max} = 600$ MeV [EPJC81(2021)1017]

The transition scattering matrices in a coupled channel formalism

[PLB742(2015)363 and EPJC81(2021)268]

$$t = [1 - VG]^{-1} V \tag{4-b}$$

with the transition potentials V_{ij} obtained from [EPJC81(2021)1017]

$$t^{(4)} = \alpha\, h \left\{ 1 + \sum_i \widetilde{W}_i\, G_i(M_{\rm inv}, \pi^- K^+)\, t_{i,\pi^- K^+}(M_{\rm inv}, \pi^- K^+) \right\} \qquad \textbf{(Fig. 4)}$$

with $i = \pi^- K^+, \pi^0 K^0$ and weights $\widetilde{W}_{\pi^- K^+} = 1$, $\widetilde{W}_{\pi^0 K^0} = -\frac{1}{\sqrt{2}}$.

$$t^{(5+6)} = \gamma\, h \left\{ 1 + \sum_i W'_i\, G_i(M_{\rm inv}, \pi\pi)\, t_{i,\pi^+\pi^-}(M_{\rm inv}, \pi\pi) \right\} \qquad \textbf{(Fig. 5+ Fig. 6)}$$

$W'_{\pi^+\pi^-} = 1$, $W'_{\pi^0\pi^0} = \frac{1}{\sqrt{2}}$, $W'_{K^+K^-} = 1$, $W'_{K^0\bar{K}^0} = 2$, $W'_{\eta\eta} = \frac{4}{3}\frac{1}{\sqrt{2}}$, $W'_{\pi^0\eta} = -\sqrt{\frac{2}{3}}$

Vector resonance production

We look to the mechanisms for K^{*0} and ρ^0 production, respectively, including their corresponding decays. In both cases, we have $K^+\pi^+\pi^-$ in the final state.

Fig. 8 (Fig. 1) produce a π^+ and K^{*0} with external emission, and $K^{*0} \to K^+\pi^-$, one important modes observed in the BESIII experiment [JHEP08(2022)196]

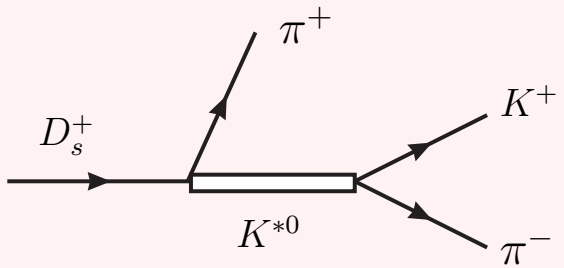

Fig. 8. Mechanism for $D_s^+ \to \pi^+ K^{*0}$, $K^{*0} \to K^+\pi^-$

Fig. 9 (Fig. 2) produce a ρ^0 meson and a K^+, and the $\rho^0 \to \pi^+\pi^-$, again one important mode observed in the BESIII experiment [JHEP08(2022)196]

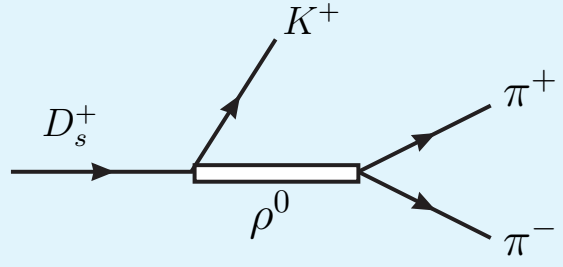

Fig. 9. Mechanism for $D_s^+ \to K^+\rho^0$, $\rho^0 \to \pi^+\pi^-$

In order to obtain the $K^{*0} \to K^+\pi^-$ and $\rho^0 \to \pi^+\pi^-$ vertices, we use the standard Lagrangian [PRL54(1985)1215; Nuovo Cim A 108 (1995) 241; Phys Rept 161 (1988) 213; PRD79(2009)014015]

The amplitudes for vector resonance production

We can write the amplitude in terms of the invariant masses s_{12}, s_{13}, s_{23} for the particles in the order $\pi^-(1), \pi^+(2), K^+(3)$.

for K^{*0} vector resonance

$$t^{(1)} = \alpha\, g \frac{1}{s_{13} - m^2_{K^*} + i m_{K^*}\Gamma_{K^*}} \left\{ -s_{23} + s_{12} + \frac{(m^2_{K^+} - m^2_{\pi^-})(m^2_{D_s} - m^2_{\pi^+})}{m^2_{K^*}} \right\}$$

(Fig. 8 / Fig. 1])

where $s_{13} = (P_{\pi^-} + P_{K^+})^2$, $s_{12} = (P_{\pi^-} + P_{\pi^+})^2$, $s_{23} = (P_{\pi^+} + P_{K^+})^2$.

for ρ^0 vector resonance

$$t^{(2)} = \gamma\, g \sqrt{2} \frac{1}{s_{12} - m^2_\rho + i\, m_\rho \Gamma_\rho} \{-s_{13} + s_{23}\}$$

(Fig. 9 / Fig. 2])

and we use the relationship

$$s_{12} + s_{23} + s_{13} = m^2_{D_s} + m^2_{K^+} + m^2_{\pi^+} + m^2_{\pi^-} .$$

The amplitudes for higher mass scalar resonances

Following the analysis of the experimental work , we also allow the contribution of two scalar resonances, the $f_0(1370)$ and $K_0^*(1430)$ [JHEP08(2022)196].

Fig. 10 production $K_0^*(1430)$ scalar resonance

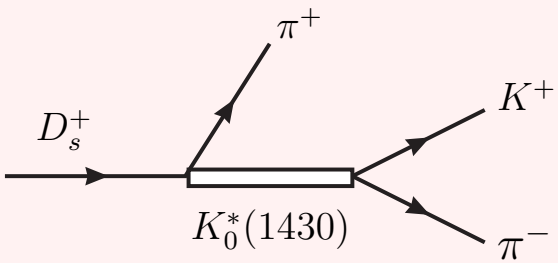

Fig. 10. Mechanism for $D_s^+ \to \pi^+ K_0^*(1430)$, $K_0^*(1430) \to K^+\pi^-$

$$t^{(7)} = \beta \frac{m_{D_s}^2}{s_{13} - m^2_{K_0^*(1430)} + i\, m_{K_0^*(1430)} \Gamma_{K_0^*(1430)}}$$

Fig. 11 production $f_0(1370)$ scalar resonance

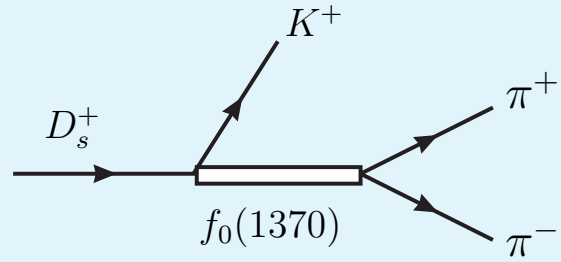

Fig. 11. Mechanism for $D_s^+ \to K^+ f_0(1370)$, $f_0(1370) \to \pi^+\pi^-$

$$t^{(8)} = \delta \frac{m_{D_s}^2}{s_{12} - m^2_{f_0(1370)} + i\, m_{f_0(1370)} \Gamma_{f_0(1370)}}$$

These resonances are obtained from vector-vector interaction in the chiral unitary approach [Molina, Nicmorus, Oset, PRD78(2008)114018; Gen, Oset, PRD79 (2009) 074009] with less precision of $150 - 200$ MeV mass difference compared with the experiment, $\Longrightarrow$ introduce them **empirically** as **free parameters**.

The sum of all amplitudes

$$t = t^{(1)} + t^{(2)} + t^{(3)} + t^{(4)} + t^{(5+6)} + t^{(7)} + t^{(8)} \tag{5}$$

We obtain the final mass distribution

$$\frac{d^2\Gamma}{dm_{12}^2 dm_{23}^2} = \frac{1}{(2\pi)^3}\frac{1}{32M_{D_s}^3}|t|^2 \tag{6}$$

where $m_{12}^2 = s_{12}$ for $\pi^+\pi^-$ and $m_{23}^2 = s_{23}$ for π^+K^+.

We integrate Eq. (6) over s_{23} with the limits of the PDG and obtain $d\Gamma/dm_{12}^2$.

By cyclical permutation of the indices we easily obtain $d\Gamma/dm_{13}^2$ and $d\Gamma/dm_{23}^2$.

Results of invariant mass distributions

$\pi^+\pi^-$, $K^+\pi^+$, $K^+\pi^-$

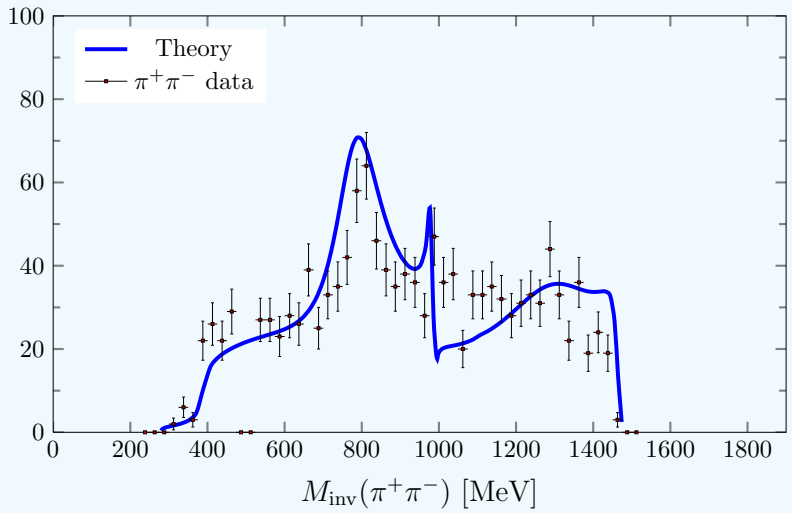

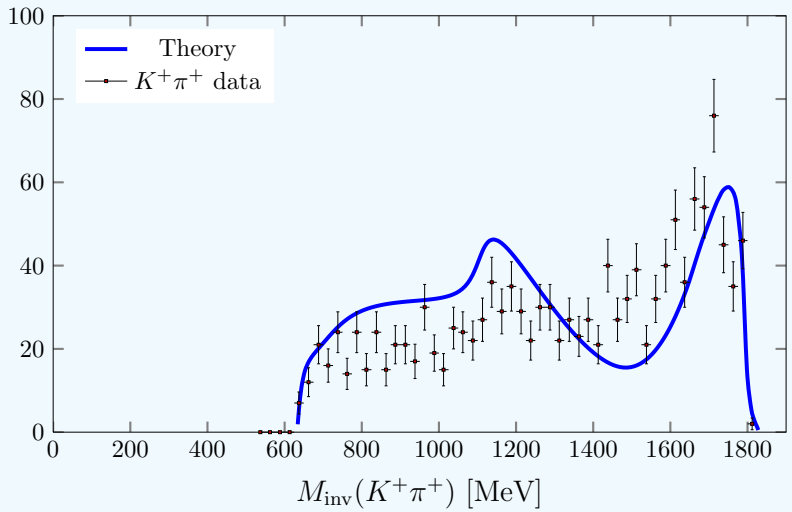

By conducting a **best fit** to the experimental data of three invariant mass distributions [JHEP08(2022)196] to obtain the parameters

$$\alpha = 14.67 \pm 1.28 \quad h = 6.86 \pm 2.57$$

$$\gamma = 10.75 \pm 2.31$$

$$\beta = -33.23 \pm 24.85 \quad \delta = -58.84 \pm 31.27$$

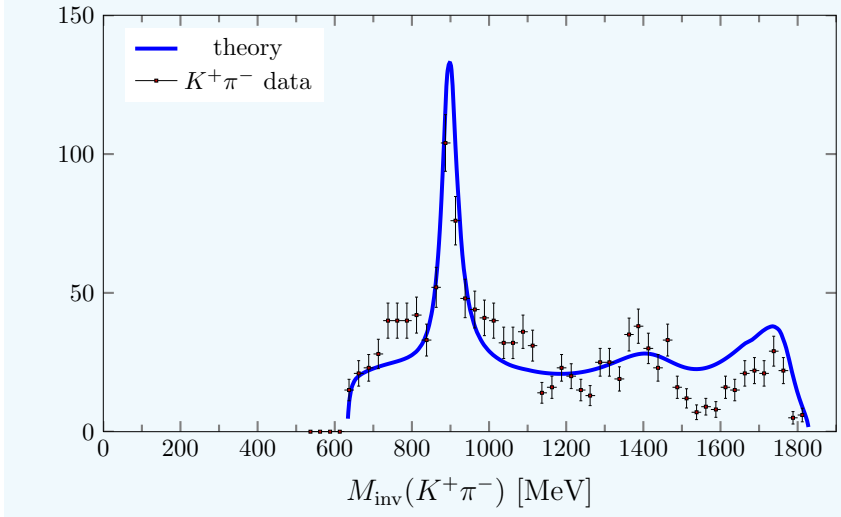

The agreement with the data is relatively fair and the K^{*0}, ρ^0 peaks are prominent in the reaction.

higher mass scalar resonances

The errors in the β and γ parameters are larger, indicating a **minor role** of the $K_0^*(1430)$ and $f_0(1370)$ resonances.

The $K_0^*(1430)$ contribution is observed as a soft peak in the $K^+\pi^-$ mass spectrum around 1400 MeV

The $f_0(1370)$, which has a very large width, shows up in the $\pi^+\pi^-$ spectrum around 1200 - 1400 MeV.

$f_0(500), f_0(980)$ and $K_0^*(700)$ resonances

which are dynamically generated through the interaction of pseudoscalar pairs in the chiral unitary approach

In the low energy part of the $\pi^+\pi^-$ mass spectrum, we can see the contributions of $f_0(500)$, the sharp peak around 980 MeV ($f_0(980)$).

In the low energy part of the $K^+\pi^-$ mass spectrum, we can see the contribution of $K_0^*(700)$.

All three resonance contributions $\Longrightarrow$ a unique parameter h

The fair reproduction of the spectra supports that these contributions are indeed correlated
our mechanism produces a fair reproduction in these three $\pi^+\pi^-$, $K^+\pi^+$, $K^+\pi^-$ mass distributions.

Test 1: keep only the K^* contribution

($t^{(1)}$ amplitude)

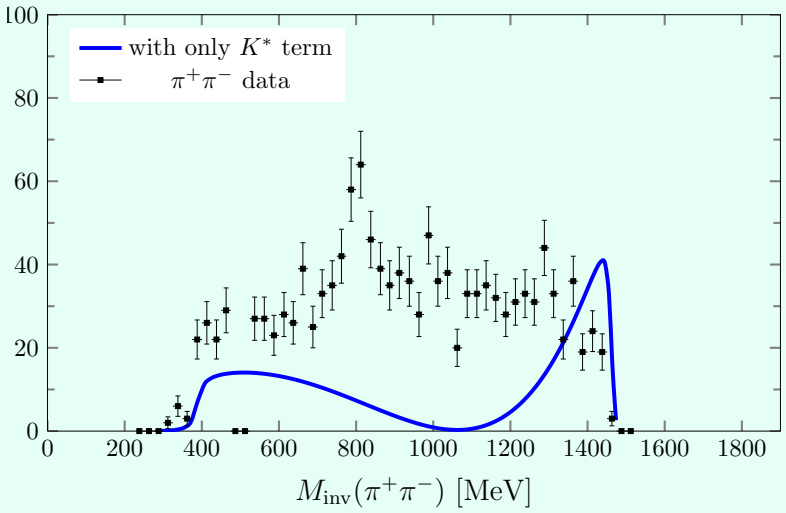

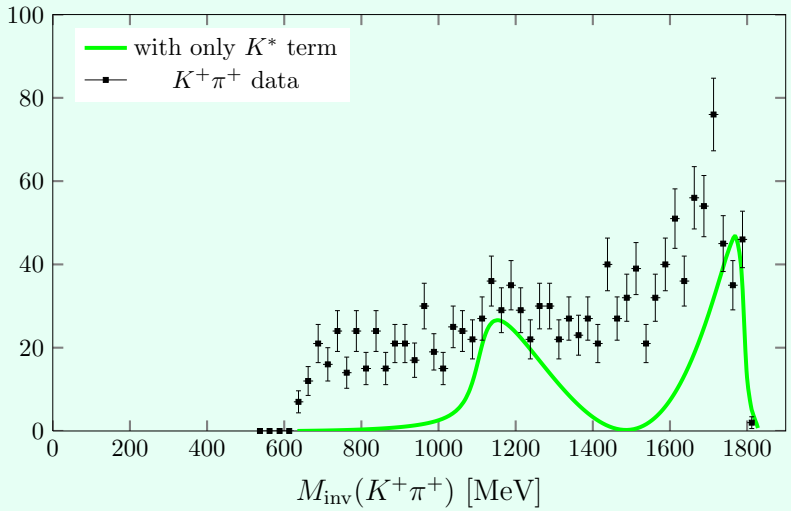

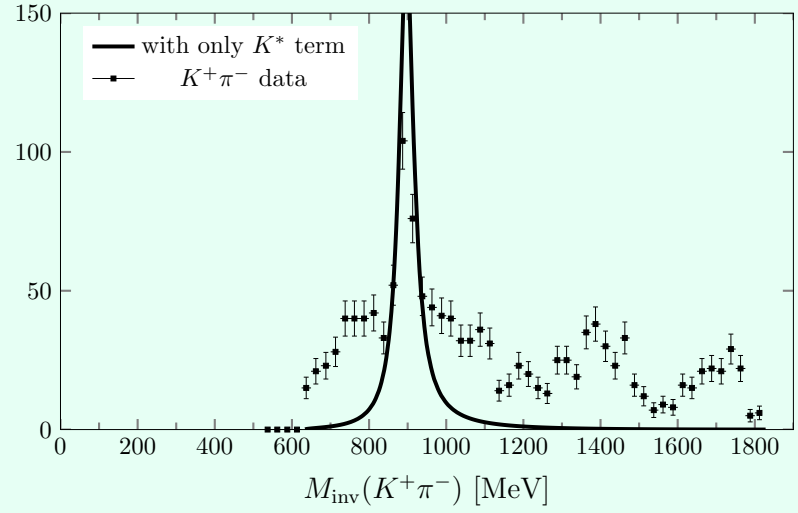

We observe that much of the strength in the $K^+\pi^-$ mass distribution outside the K^{*0} peak is not accounted for.

It produces a two peak structure in the $K^+\pi^+$ distribution and also in the $\pi^+\pi^-$ one.

These peaks are well known as reflections and not signals of a new resonance.

Test 2: keep only the ρ contribution

($t^{(2)}$ amplitude)

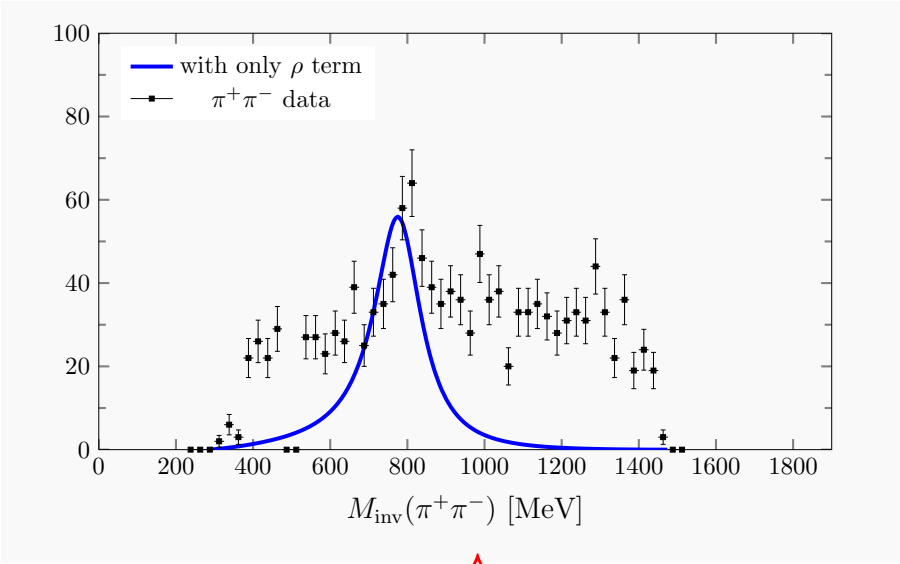

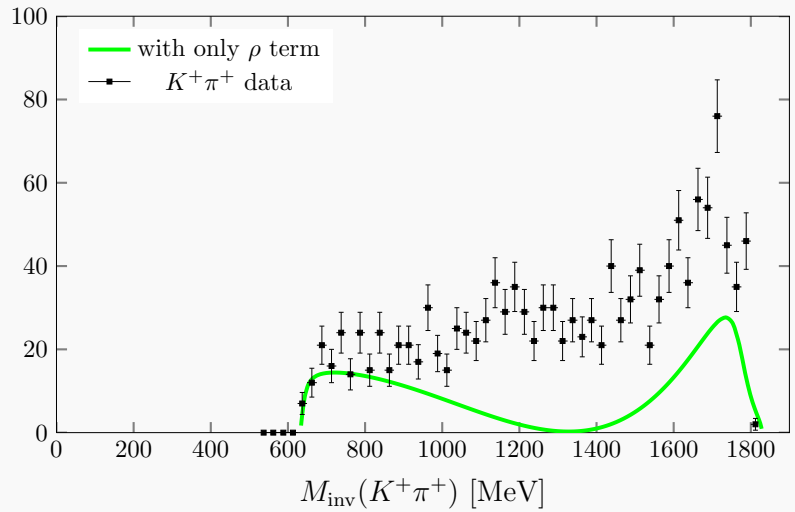

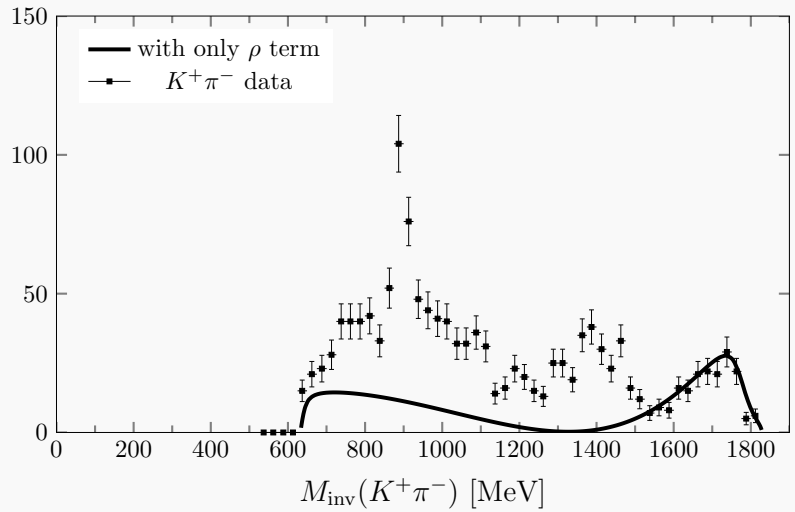

Once again, we show that much strength outside the ρ in the $\pi^+\pi^-$ region is not accounted for.

The ρ peak generates reflections with two peaks, both in the $K^+\pi^+$ and $K^+\pi^-$ mass distributions.

again reflections

Summary

1. In the same $D_s^+ \to K^+\pi^+\pi^-$ reaction, we have performed a fit to the three $\pi^+\pi^-$, $K^+\pi^+$, $K^+\pi^-$ mass distributions.

2. Introduced empirically

$$\begin{cases} D_s^+ \to K^+\rho^0\,, D_s^+ \to K^{*0}\pi^0 & \textbf{main decay channels} \\ D_s^+ \to \pi^+ K_0^*(1430)\,, D_s^+ \to K^+ f_0(1370) & \textbf{smaller relevance} \end{cases}$$

3. For light $f_0(500)$, $f_0(980)$ and $K_0^*(700)$ scalar resonances, **introduced dynamically** and their contributions are correlated by means of **just one free parameter**.

We obtain a fair reproduction of the $\pi^+\pi^-$, $K^+\pi^-$ mass distributions, the relative weight of the contribution also agrees with the measured spectra.

Reproducing their effect by means of just one parameter adds **extra support** for the dynamically generated origin of these resonances, stemming from the interaction of pseudoscalar mesons.

Thank you（谢谢）